Journal of Applied Mechanics and Technical Physics, Vol. 48, No. 3, pp. 401–411, 2007

NUMERICAL SIMULATION OF PLASMA MOTION IN A MAGNETIC FIELD. TWO-DIMENSIONAL CASE

V. T. Astrelin,[1] V. M. Kovenya,[2] and T. V. Kozlinskaya[3]

UDC 517.958:537.84

A model of dynamics and heating of a plasma cloud in a magnetic field is considered in a two-temperature approximation. Based on a predictor–corrector-type implicit difference scheme, spreading of a plasma cloud in an external magnetic field is numerically simulated, and the influence of this field on spread dynamics is evaluated.

Key words: *plasma physics, difference scheme, splitting method, numerical simulation.*

Introduction. In experiments on plasma heating and confinement in a multiple-mirror trap in a GOL-3 setup, rapid heating of the plasma can be ensured by using a relativistic electron beam. Experiments demonstrated that the electron component of the plasma is heated under conditions of a developed Langmuir turbulence suppressing electron-type heat conduction. Rapid heating of ions in the plasma to a temperature commensurable with the electron temperature is observed thereby. This heating can be attributed to a collective character of ion acceleration under the gradient of the electron pressure of the plasma rather than to electron–ion collisions [1, 2]. To study the above-described mechanism of fast transfer of energy from electrons to ions, Arzhannikov et al. [3] and Astrelin et al. [4] modeled the dynamics of a two-component plasma in a one-dimensional hydrodynamic approximation by different numerical methods. Numerical and experimental results show that plasma motion under these conditions is accompanied by emergence of high-amplitude nonlinear waves. This required a special numerical method to be developed [4, 5], which would be stable in a wide range of plasma parameters and sufficiently accurate for solving problems of this class.

A refined two-dimensional model is proposed in the present paper to describe the motion of a one-fluid two-temperature plasma with allowance for the effects of heat conduction, electrical conduction, thermal forces, and friction forces arising in collisions between ions and electrons. A predictor–corrector-type implicit difference scheme was proposed for the numerical solution of magnetohydrodynamic problems in one-dimensional and multidimensional approximations [5, 6]. This model is extended below to the case of a two-temperature plasma. The problem of spreading of an originally spherical hot plasma cloud under the action of hydrodynamic forces and a magnetic field is solved. At the present stage of research, dissipative effects are neglected, but it is assumed that the initial ion and electron temperatures may be different. The influence of an external magnetic field and initial temperature distribution within wide ranges of their values on the characteristics of plasma motion is studied.

Physicomathematical Model. The problem of propagation of a dense plasma cloud in an external magnetic field is considered. The original plasma cloud is assumed to have a spherical shape and to have parameters (pressure, density, and temperature) whose values are several orders higher than the background level. Under the action of hydrodynamic and magnetic pressures, this cloud starts spreading over the background plasma. The flow is assumed to be axisymmetric and is simulated as propagation of a plasma cloud in a certain volume in the presence of an external magnetic field. In the magnetohydrodynamic approximation, the system of equations of

[1]Budker Institute of Nuclear Physics, Siberian Division, Russian Academy of Sciences, Novosibirsk 630090. [2]Institute of Computational Technologies, Siberian Division, Russian Academy of Sciences, Novosibirsk 630090; kovenya@ict.nsc.ru. [3]Novosibirsk State University, Novosibirsk 630090; ktv-sun@mail.ru. Translated from Prikladnaya Mekhanika i Tekhnicheskaya Fizika, Vol. 48, No. 3, pp. 121–132, May–June, 2007. Original article submitted January 9, 2007.

plasma motion contains equations of continuity, motion, magnetic field, and thermal balance for electrons and ions; in the vector form, the system is [6]

$$\frac{\partial n}{\partial t} + \operatorname{div}(n\boldsymbol{v}) = 0, \qquad m_i n \frac{d\boldsymbol{v}}{dt} = -\nabla p + \frac{1}{c}(\boldsymbol{j} \times \boldsymbol{B}),$$

$$\frac{1}{\gamma - 1} n \frac{dT_i}{dt} + p_i \operatorname{div} \boldsymbol{v} = -\operatorname{div} \boldsymbol{q}_i + \frac{3m_e}{m_i \tau_e}(p_e - p_i),$$

$$\frac{1}{\gamma - 1} n \frac{dT_e}{dt} + p_e \operatorname{div} \boldsymbol{v} = -\operatorname{div} \boldsymbol{q}_e + \frac{j_\parallel^2}{\sigma_\parallel} + \frac{j_\perp^2}{\sigma_\perp} + \frac{1}{en} \boldsymbol{j} \cdot \boldsymbol{R}_T - \frac{3m_e}{m_i \tau_e}(p_e - p_i), \tag{1}$$

$$\frac{\partial \boldsymbol{B}}{\partial t} = \operatorname{rot}(\boldsymbol{v} \times \boldsymbol{B}) - \operatorname{rot}\left(\frac{\boldsymbol{j}}{en} \times \boldsymbol{B}\right) - \frac{c}{en}(\nabla n \times \nabla T) - \frac{c}{e} \operatorname{rot} \frac{\boldsymbol{R}_T}{n} - c \operatorname{rot}\left(\frac{\boldsymbol{j}_\parallel}{\sigma_\parallel} + \frac{\boldsymbol{j}_\perp}{\sigma_\perp}\right).$$

Here $d/dt = \partial/\partial t + (\boldsymbol{v} \cdot \nabla)$, t is the time, n and $\boldsymbol{v}$ are the plasma density and velocity, T_e and T_i are the electron and ion temperatures, $\boldsymbol{B}$ is the magnetic field vector, c is the velocity of sound, e is the electron charge, m_e and m_i are the electron and ion masses, $\boldsymbol{q}_i$ and $\boldsymbol{q}_e$ are the ion and electron fluxes defined by the relations

$$\boldsymbol{q}_i = -\varkappa_\parallel^i \nabla_\parallel T_i - \varkappa_\perp^i \nabla_\perp T_i + \frac{5}{2} \frac{cp_i}{eB}(\boldsymbol{h} \times \nabla T_i),$$

$$\boldsymbol{q}_e = -\varkappa_\parallel^e \nabla_\parallel T_i - \varkappa_\perp^e \nabla_\perp T_i - \frac{5}{2} \frac{cp_e}{eB}(\boldsymbol{h} \times \nabla T_e) + 0.71 p_e u_\parallel - \frac{3}{2} \frac{p_e}{\omega_e \tau_e}(\boldsymbol{h} \times \boldsymbol{u}),$$

$\boldsymbol{h} = \boldsymbol{B}/B$ is the unit vector along the magnetic field, $\varkappa_\parallel^i = 3.9 p_i \tau_i / m_i$, $\varkappa_\parallel^e = 3.16 p_e \tau_e / m_e$, $\varkappa_\perp^i = 2 p_i T_e / (m_i \omega_i^2 \tau_i)$, and $\varkappa_\perp^e = 4.66 p_e / (m_e \omega_e^2 \tau_e)$ are the longitudinal and transverse thermal conductivities for ions and electrons, $\boldsymbol{j} = (c/(4\pi)) \operatorname{rot} \boldsymbol{B}$ is the current density, $\omega_{i,e} = eB/(m_{i,e}c)$ are the cyclotron frequencies of electrons and ions, $\boldsymbol{a}_\parallel = \boldsymbol{h}(\boldsymbol{a} \cdot \boldsymbol{h})$ and $\boldsymbol{a}_\perp = \boldsymbol{h} \times (\boldsymbol{a} \times \boldsymbol{h})$ are the components of the vector $\boldsymbol{a}$, which are parallel and perpendicular to the magnetic field, $\boldsymbol{u} = -\dfrac{1}{en}\boldsymbol{j}$, $\tau_e = \dfrac{3.5 \cdot 10^4}{\lambda/10} \dfrac{T_e^{3/2}}{n}$ and $\tau_i = \dfrac{3 \cdot 10^6}{\lambda/10} \sqrt{\dfrac{m_i}{2m_p}} \dfrac{T_i^{3/2}}{n}$ are the "times between the collisions" of electrons and ions, $\sigma_1 = 9 \cdot 10^{12}/(\lambda/10)$, $\sigma_\parallel = 1.96 \sigma_1 T_e^{3/2}$, and $\sigma_\perp = \sigma_1 T_e^{3/2}$ are the electrical conductivities, λ is the Coulomb logarithm: $\lambda = 23.4 - 1.15 \log n + 3.45 \log T_e$ for $T_e \leqslant 50$ eV and $\lambda = 25.3 - 1.15 \log n + 2.3 \log T_e$ for $T_e > 50$ eV; $\boldsymbol{R}_T = -0.71 n \nabla_\parallel T_e - \dfrac{3}{2} \dfrac{n}{\omega_e \tau_\varepsilon}(h \times \nabla T_e)$ is the thermal force.

System (1) is closed by the equation of state in the form

$$p_e = nT_e, \qquad p_i = nT_i, \qquad p = p_e + p_i \tag{2}$$

and by the relation

$$\operatorname{div} \boldsymbol{B} = \frac{1}{r} \frac{\partial}{\partial r}(rB_r) + \frac{\partial B_z}{\partial z} = 0. \tag{3}$$

The flow is assumed to be symmetric with respect to the angular coordinate, i.e., $\partial/\partial\varphi = 0$. The solution of the equations is independent of the angular coordinate but contains all components of velocity and magnetic field in the directions of the cylindrical coordinate system z, r, and φ.

For convenience of numerical simulation and analysis of results, Eqs. (1) can be written in dimensionless form by setting the length L, velocity U_0, magnetic field B_0, plasma density n_0, and temperature T_0 as dimensionless parameters. The sought functions are the plasma density, velocity components, ion and electron pressures, and magnetic field components. Then, system (1)–(3) in the cylindrical coordinate system can be presented in dimensionless form as

$$\frac{\partial n}{\partial t} + \frac{1}{r} \frac{\partial}{\partial r}(rnv_r) + \frac{\partial}{\partial z}(nv_z) = 0,$$

$$\frac{\partial}{\partial t}(nv_r) + \frac{1}{r} \frac{\partial}{\partial r}(rnv_r^2) + \frac{\partial}{\partial z}(nv_r v_z) - \frac{nv_\varphi^2}{r} + k_0 \frac{\partial p}{\partial r} - M(j_\varphi B_z - j_z B_\varphi) = 0,$$

$$\frac{\partial}{\partial t}(nv_\varphi) + \frac{1}{r} \frac{\partial}{\partial r}(rnv_r v_\varphi) + \frac{\partial}{\partial z}(nv_r v_\varphi) + \frac{nv_\varphi v_r}{r} - M(j_z B_r - j_r B_z) = 0,$$

$$\frac{\partial}{\partial t}(nv_z)+\frac{1}{r}\frac{\partial}{\partial r}(rnv_rv_z)+\frac{\partial}{\partial z}(nv_rv_z)+k_0\frac{\partial p}{\partial z}-M(j_rB_\varphi-j_\varphi B_r)=0,$$

$$\frac{\partial p_e}{\partial t}+\frac{1}{r}\frac{\partial}{\partial r}(rv_rp_e)+\frac{\partial}{\partial z}(v_zp_e)+lp_e\Big(\frac{1}{r}\frac{\partial}{\partial r}rv_r+\frac{\partial v_z}{\partial z}\Big)+k(p_e-p_i)$$
$$=\frac{1}{r}\frac{\partial}{\partial r}r\Big(\varkappa^e_{rr}\frac{\partial T_e}{\partial r}+\varkappa^e_{rz}\frac{\partial T_e}{\partial z}\Big)+\frac{\partial}{\partial z}\Big(\varkappa^e_{zr}\frac{\partial T_e}{\partial r}+\varkappa^e_{zz}\frac{\partial T_e}{\partial z}\Big)$$
$$+lM\Big[\sigma_1(j^2-j_0^2k_0)+\varphi\Big(\frac{1}{r}\frac{\partial}{\partial r}ra_1T_e+\frac{\partial}{\partial z}a_2T_e+b_1\frac{\partial T_e}{\partial r}+b_2\frac{\partial T_e}{\partial z}\Big)\Big], \tag{4}$$

$$\frac{\partial p_i}{\partial t}+\frac{1}{r}\frac{\partial}{\partial r}(rv_rp_i)+\frac{\partial}{\partial z}(v_zp_i)+lp_i\Big(\frac{1}{r}\frac{\partial}{\partial r}rv_r+\frac{\partial v_z}{\partial z}\Big)-k(p_e-p_i)$$
$$=\frac{1}{r}\frac{\partial}{\partial r}r\Big(\varkappa^i_{rr}\frac{\partial T_i}{\partial r}+\varkappa^i_{rz}\frac{\partial T_i}{\partial z}\Big)+\frac{\partial}{\partial z}\Big(\varkappa^i_{zr}\frac{\partial T_i}{\partial r}+\varkappa^i_{zz}\frac{\partial T_i}{\partial z}\Big),$$

$$\frac{\partial B_r}{\partial t}=\frac{\partial}{\partial z}(v_rB_z-v_zB_r)-\varphi\Big[\frac{\partial}{\partial z}\Big(d_1\frac{\partial T_e}{\partial r}+d_2\frac{\partial T_e}{\partial z}\Big)+M\frac{\partial}{\partial z}\frac{1}{n}(j_zB_r-j_rB_z)\Big]$$
$$-\frac{\partial}{\partial z}(\mu_{r\varphi}j_r+\mu_{\varphi\varphi}j_\varphi+\mu_{\varphi z}j_z),$$

$$\frac{\partial B_\varphi}{\partial t}=\frac{\partial}{\partial z}(v_\varphi B_z-v_zB_\varphi)-\frac{\partial}{\partial r}(v_rB_\varphi-v_\varphi B_r)$$
$$+\varphi\Big\{\frac{\partial}{\partial z}\Big(d_3\frac{\partial T_e}{\partial r}+d_4\frac{\partial T_e}{\partial z}\Big)-\frac{\partial}{\partial r}\Big(d_5\frac{\partial T_e}{\partial r}+d_6\frac{\partial T_e}{\partial z}\Big)-\frac{1}{n}\Big(\frac{\partial n}{\partial z}\frac{\partial T}{\partial z}-\frac{\partial n}{\partial r}\frac{\partial T}{\partial z}\Big)$$
$$+M\Big[-\frac{\partial}{\partial z}\frac{1}{n}(j_\varphi B_z-j_zB_\varphi)+\frac{\partial}{\partial r}\frac{1}{n}(j_rB_\varphi-j_\varphi B_r)\Big]\Big\}$$
$$+\frac{\partial}{\partial z}(\mu_{rr}j_r+\mu_{r\varphi}j_\varphi+\mu_{rz}j_z)-\frac{\partial}{\partial r}(\mu_{rz}j_r+\mu_{\varphi z}j_\varphi+\mu_{zz}j_z),$$

$$\frac{\partial B_z}{\partial t}=\frac{1}{r}\frac{\partial}{\partial r}r(v_zB_r-v_rB_z)+\frac{1}{r}\frac{\partial}{\partial r}r(\mu_{r\varphi}j_r+\mu_{\varphi\varphi}j_\varphi+\mu_{\varphi z}j_z)$$
$$+\frac{\varphi}{r}\Big\{\frac{\partial}{\partial r}r\Big(d_1\frac{\partial T_e}{\partial r}+d_2\frac{\partial T_e}{\partial z}\Big)-M\frac{\partial}{\partial r}\frac{r}{n}(j_rB_z-j_zB_r)\Big\}.$$

Here

$$M=M_{\rm A}^2=\frac{B_0^2}{4\pi m_in_0U_0^2};\quad k_0=\frac{T_0}{U_0^2m_i};\quad k=\frac{3lm_eL}{m_i\tau_eU_0};\quad \sigma=T_e^{3/2};\quad \sigma_0=\frac{9\cdot10^{12}}{\lambda/10};$$

$$\sigma_1=\frac{1}{{\rm Re}_m}=\frac{c^2\sigma}{4\pi LU_0\sigma_0};\quad j_r=-\frac{\partial B_\varphi}{\partial z};\quad j_\varphi=\frac{\partial B_r}{\partial z}-\frac{\partial B_z}{\partial r};\quad j_z=\frac{1}{r}\frac{\partial}{\partial r}(rB_\varphi);$$

$$k_1=1-\frac{\sigma_\perp}{\sigma_\parallel}=\frac{0{,}96}{1{,}96};\quad k_2=\frac{1}{l\omega_e\tau_e};\quad \varphi=\frac{c_0T_0}{eB_0LU_0};$$

$$\bar\varkappa^e_\perp=\frac{4{,}66nT_e}{m_e\tau_e\omega_e^2};\quad \bar\varkappa^e_\parallel=\frac{3{,}16nT_e\tau_e}{m_e};\quad \bar\varkappa^i_\perp=\frac{2nT_i}{Zm_i\tau_i\omega_i^2};\quad \bar\varkappa^i_\parallel=\frac{3{,}9nT_i\tau_i}{Zm_i};$$

$$k_1^i=\frac{l\bar\varkappa^i_\perp}{n_0LU_0};\qquad k_1^e=\frac{l\bar\varkappa^e_\perp}{n_0LU_0};$$

$$d_1=sh_\varphi h_r+\psi h_z;\quad d_2=sh_\varphi h_z-\psi h_r;\quad d_3=sh_r^2;$$

$$d_4=sh_rh_z+\psi h_\varphi;\quad d_5=sh_zh_r-\psi h_\varphi;\quad d_6=sh_z^2;\quad s=0{,}71;$$

$$\psi_0 = \psi(j_z h_\varphi - j_\varphi h_z); \quad \psi_1 = \psi(j_\varphi h_r - j_r h_\varphi);$$

$$j_0 = j_r h_r + j_\varphi h_\varphi + j_z h_z; \quad j_1 = s j_0;$$

$$\varkappa_{rr}^{i,e} = h_r^2 \varkappa^{i,e} + \varkappa_1^{i,e}; \quad \varkappa_{zz}^{i,e} = h_z^2 \varkappa^{i,e} + \varkappa_1^{i,e};$$

$$\varkappa_{rz}^{i,e} = h_r h_z \varkappa_1^{i,e} \mp \varkappa_0^{i,e} h_\varphi; \quad \varkappa_{zr}^{i,e} = h_r h_z \varkappa_1^{i,e} \pm \varkappa_0^{i,e} h_\varphi;$$

$$\varkappa_1^{i,e} = k_1^{i,e} \varkappa_\perp^{i,e}; \quad \varkappa_2^{i,e} = k_2^{i,e} \varkappa_\parallel^{i,e}; \quad \varkappa_0^{i,e} = \gamma\varphi(\varkappa_2^{i,e} - \varkappa_1^{i,e}); \quad \varkappa_\parallel^{i,e} = T_{i,e}^{5/2}; \quad \varkappa_\perp^{i,e} = \frac{n}{B T_{i,e}^{1/2}};$$

$$a_1 = j h_r + \psi_0; \quad a_2 = j_1 h_z + \psi_1; \quad b_1 = -j_1 h_r + \psi_0; \quad b_2 = -j_1 h_z + \psi_1;$$

$$\mu_{rr} = \sigma_1(k_1 h_r^2 - 1); \quad \mu_{\varphi\varphi} = \sigma_1(k_1 h_\varphi^2 - 1); \quad \mu_{zz} = \sigma_1(k_1 h_z^2 - 1);$$

$$\mu_{r\varphi} = k_1 \sigma_1 h_\varphi h_r; \quad \mu_{rz} = k_1 \sigma_1 h_r h_z; \quad \mu_{\varphi z} = k_1 \sigma_1 h_\varphi h_z.$$

The boundary conditions are set as follows. At the initial time, the background values of the plasma in the entire computational domain, except for the plasma cloud of diameter d, are

$$\begin{gathered} n = 1, \quad v_r = 0, \quad v_\varphi = 0, \quad v_z = 0, \\ p_e = p_{e,\text{in}}, \quad p_i = p_{i,\text{in}}, \quad B_r = 0, \quad B_\varphi = 0, \quad B_z = 1, \end{gathered} \tag{5}$$

and the background values in the plasma cloud with $\sqrt{r^2 + z^2} \leqslant d$ are

$$\begin{gathered} n = n_{\text{cl}}, \quad v_r = 0, \quad v_\varphi = 0, \quad v_z = 0, \\ p_e = p_{e,\text{cl}}, \quad p_i = p_{i,\text{cl}}, \quad B_r = 0, \quad B_\varphi = 0, \quad B_z = 1. \end{gathered} \tag{6}$$

The calculations were normally performed until the disturbances from the cloud reached the boundaries [otherwise, soft boundary conditions (outflow conditions) were set at these boundaries]. The solution of the problem was found for the upper half-plane; hence, by virtue of the problem symmetry, the following conditions were set at the axis $r = 0$:

$$\frac{\partial n}{\partial z} = v_r = v_\varphi = \frac{\partial v_z}{\partial z} = \frac{\partial p_e}{\partial z} = \frac{\partial p_i}{\partial z} = \frac{\partial B_r}{\partial z} = B_\varphi = \frac{\partial B_z}{\partial z} = 0. \tag{7}$$

The solution of Eqs. (4) with the boundary conditions (5)–(7) was found numerically by a predictor–corrector difference scheme [5] with splitting in terms of the spatial directions and special splitting of one-dimensional operators in terms of the physical processes. Let us briefly describe the principles of constructing this scheme for system (4) without dissipative terms. Let us write system (4) as a differential scheme in conservative form:

$$\frac{\partial \boldsymbol{U}}{\partial t} = \boldsymbol{W}, \qquad \boldsymbol{W} = -\sum_{j=1}^{2} \frac{\partial \boldsymbol{W}_j}{\partial x_j} \tag{8}$$

($\boldsymbol{U}$ and $\boldsymbol{W}_j$ are the vectors of the sought functions and fluxes in the direction x_j; $x_1 = z$ and $x_2 = r$). Then, we write this system in nondivergent form with respect to the vector of the sought functions $\boldsymbol{f}$:

$$\frac{\partial \boldsymbol{f}}{\partial t} + \sum_{j=1}^{2} B_j \frac{\partial \boldsymbol{f}}{\partial x_j} = 0. \tag{9}$$

Here $\boldsymbol{f} = (n, v_z, v_r, v_\varphi, p_e, p_i, B_z, B_r, B_\varphi)^{\text{t}}$; B_j are the differential matrix operators in each spatial direction. We introduce splitting of one-dimensional matrix operators into a sum of matrices of simpler structure $B_j = B_j^1 + B_j^2$ so that the difference scheme for the split equations

$$\frac{\partial \boldsymbol{f}}{\partial t} + B_j^i \frac{\partial \boldsymbol{f}}{\partial x_j} = 0 \qquad (i, j = 1, 2)$$

is implemented by effective algorithms (e.g., scalar sweeps for each component of the vector $\boldsymbol{f}$), and additional terms of the form $B_j^l \cdot B_j^s$ ($s \neq l$) arising owing to splitting have a minimum number of nonzero elements [5]. Then, system (9) can be presented as

$$\frac{\partial \boldsymbol{f}}{\partial t} + \sum_{j=1}^{2}\sum_{i=1}^{2} B_j^i \boldsymbol{f} = 0,$$

where the matrices B_j^i in the cylindrical coordinate system ($x_1 = z$, $x_2 = r$) are

$$B_1^1 = \begin{pmatrix}
\frac{1}{r}\frac{\partial}{\partial r} r v_r & 0 & 0 & 0 & 0 & 0 & 0 & 0 & 0 \\
0 & v_r \frac{\partial}{\partial r} & 0 & 0 & \frac{k_0}{n}\frac{\partial}{\partial r} & \frac{k_0}{n}\frac{\partial}{\partial r} & 0 & \frac{MB_\varphi}{rn}\frac{\partial}{\partial r} r & \frac{MB_z}{n}\frac{\partial}{\partial r} \\
0 & 0 & v_r \frac{\partial}{\partial r} & 0 & 0 & 0 & 0 & 0 & 0 \\
0 & 0 & 0 & v_r \frac{\partial}{\partial r} & 0 & 0 & 0 & 0 & 0 \\
0 & \frac{\gamma p_e}{r}\frac{\partial}{\partial r} r & 0 & 0 & 0 & 0 & 0 & 0 & 0 \\
0 & \frac{\gamma p_i}{r}\frac{\partial}{\partial r} r & 0 & 0 & 0 & 0 & 0 & 0 & 0 \\
0 & 0 & 0 & 0 & 0 & 0 & 0 & 0 & 0 \\
0 & B_\varphi \frac{\partial}{\partial r} & 0 & 0 & 0 & 0 & 0 & 0 & 0 \\
0 & B_z \frac{\partial}{\partial r} & 0 & 0 & 0 & 0 & 0 & 0 & 0
\end{pmatrix},$$

$$B_1^2 = \begin{pmatrix}
0 & 0 & 0 & 0 & 0 & 0 & 0 & 0 & 0 \\
0 & 0 & -\frac{v_\varphi}{r} & 0 & 0 & 0 & 0 & 0 & 0 \\
0 & \frac{v_\varphi}{r} & 0 & 0 & 0 & 0 & 0 & -\frac{MB_r}{nr}\frac{\partial}{\partial r} r & 0 \\
0 & 0 & 0 & 0 & 0 & 0 & 0 & 0 & -\frac{MB_r}{n}\frac{\partial}{\partial r} \\
0 & 0 & 0 & 0 & v_r \frac{\partial}{\partial r} + k & -k & 0 & 0 & 0 \\
0 & 0 & 0 & 0 & 0 & v_r \frac{\partial}{\partial r} & 0 & 0 & 0 \\
0 & 0 & 0 & 0 & 0 & 0 & 0 & 0 & 0 \\
0 & 0 & -\frac{\partial}{\partial r} B_r & 0 & 0 & 0 & 0 & v_r \frac{\partial}{\partial r} & 0 \\
0 & 0 & 0 & -\frac{B_r}{r}\frac{\partial}{\partial r} r & 0 & 0 & 0 & 0 & \frac{v_r}{r}\frac{\partial}{\partial r} r
\end{pmatrix},$$

$$B_2^1 = \begin{pmatrix}
v_z \frac{\partial}{\partial z} & 0 & 0 & 0 & 0 & 0 & 0 & 0 & 0 \\
0 & v_z \frac{\partial}{\partial z} & 0 & 0 & 0 & 0 & 0 & 0 & 0 \\
0 & 0 & v_z \frac{\partial}{\partial z} & 0 & 0 & 0 & 0 & 0 & 0 \\
0 & 0 & 0 & v_z \frac{\partial}{\partial z} & \frac{k_0}{n}\frac{\partial}{\partial z} & \frac{k_0}{n}\frac{\partial}{\partial z} & \frac{MB_r}{n}\frac{\partial}{\partial z} & \frac{MB_\varphi}{n}\frac{\partial}{\partial z} & 0 \\
0 & 0 & 0 & \gamma p_e \frac{\partial}{\partial z} & 0 & 0 & 0 & 0 & 0 \\
0 & 0 & 0 & \gamma p_i \frac{\partial}{\partial z} & 0 & 0 & 0 & 0 & 0 \\
0 & 0 & 0 & B_r \frac{\partial}{\partial z} & 0 & 0 & 0 & 0 & 0 \\
0 & 0 & 0 & B_\varphi \frac{\partial}{\partial z} & 0 & 0 & 0 & 0 & 0 \\
0 & 0 & 0 & 0 & 0 & 0 & 0 & 0 & 0
\end{pmatrix},$$

$$B_2^2 = \begin{pmatrix} 0 & 0 & 0 & 0 & 0 & 0 & 0 & 0 & 0 \\ 0 & 0 & 0 & 0 & 0 & 0 & -\dfrac{MB_z}{n}\dfrac{\partial}{\partial z} & 0 & 0 \\ 0 & 0 & 0 & 0 & 0 & 0 & 0 & -\dfrac{MB_z}{n}\dfrac{\partial}{\partial z} & 0 \\ 0 & 0 & 0 & 0 & 0 & 0 & 0 & 0 & 0 \\ 0 & 0 & 0 & 0 & v_z\dfrac{\partial}{\partial z} & 0 & 0 & 0 & 0 \\ 0 & 0 & 0 & 0 & -k & v_z\dfrac{\partial}{\partial z}+k & 0 & 0 & 0 \\ 0 & -\dfrac{\partial}{\partial z}B_z & 0 & 0 & 0 & 0 & v_z\dfrac{\partial}{\partial z} & 0 & 0 \\ 0 & 0 & -\dfrac{\partial}{\partial z}B_z & 0 & 0 & 0 & 0 & v_z\dfrac{\partial}{\partial z} & 0 \\ 0 & 0 & 0 & 0 & 0 & 0 & 0 & 0 & 0 \end{pmatrix}.$$

We approximate the first derivatives ∂/x_j by difference operators Λ_j with an order $O(h_j^k)$. We introduce difference operators $B_{jh}^l\Lambda_j = B_j^l + O(h_j^k)$ approximating the corresponding difference operators with an order k. Then, for $\alpha = 0.5 + O(\tau)$, the predictor–corrector difference scheme

$$\begin{aligned} &\frac{\boldsymbol{f}^{n+1/8} - \boldsymbol{f}^n}{\tau\alpha} + B_{1h}^1\Lambda_1\boldsymbol{f}^{n+1/8} = 0, \\ &\frac{\boldsymbol{f}^{n+1/4} - \boldsymbol{f}^{n+1/8}}{\tau\alpha} + B_{1h}^2\Lambda_1\boldsymbol{f}^{n+1/4} = 0, \\ &\frac{\boldsymbol{f}^{n+3/8} - \boldsymbol{f}^{n+1/4}}{\tau\alpha} + B_{2h}^1\Lambda_2\boldsymbol{f}^{n+3/8} = 0, \\ &\frac{\boldsymbol{f}^{n+1/2} - \boldsymbol{f}^{n+3/8}}{\tau\alpha} + B_{2h}^1\Lambda_2\boldsymbol{f}^{n+1/2} = 0, \\ &\frac{\boldsymbol{U}^{n+1} - \boldsymbol{U}^n}{\tau} + \sum_{j=1}^{2}\Lambda_j\boldsymbol{W}_{jh}^{n+1/2} = 0 \end{aligned} \tag{10}$$

approximates the original equations (8) in divergent form with an order $O(\tau^2 + h_1^k + h_2^k)$. The structure of the split matrices B_j^l was chosen so that the system of difference equations (10), like the scheme developed in [6], at each fractional step could be solved by scalar sweeps for each component of the vector $\boldsymbol{f}^{n+l/8}$ (by eliminating other components of the vector from this equation). Note that the number of scalar sweeps in each spatial direction in scheme (10) is not greater than the number of the original equations. At the corrector stage, the scheme is implemented explicitly. A linear analysis of stability shows that the difference scheme (10) is absolutely stable if the above-described form of splitting is chosen. The calculations supported the theoretical estimates of stability, which allowed us to vary the scheme parameters (time and space steps of the grid) and physical parameters of the problem within wide limits in the numerical experiments.

Results of Numerical Simulations. Using the difference scheme (10), we calculated the problem of spreading of a plasma cloud. By virtue of problem symmetry, we calculated only 1/4 of the domain. In the first series of calculations, we set a pressure jump $p_{e,\mathrm{cl}} = p_{i,\mathrm{cl}} = 10^3 p_{\mathrm{in}}$, which was three orders greater than the background pressure, in the region $r_0 = \sqrt{r^2 + z^2} \leqslant 0.1$. We considered propagation of the plasma cloud with time for different values of the magnetic field (different values of M_{A}) and initial ion and electron temperatures. The numerical solution was found by scheme (10) with a weight parameter $\alpha = 0.505$ on computational grids containing 100 or 200 nodes in each spatial direction. Figure 1 shows the plasma spread at the time $t = 0.3$ for different values of n_{cl}. Under the action of the initial pressure gradient, the cloud starts spreading, and two density waves

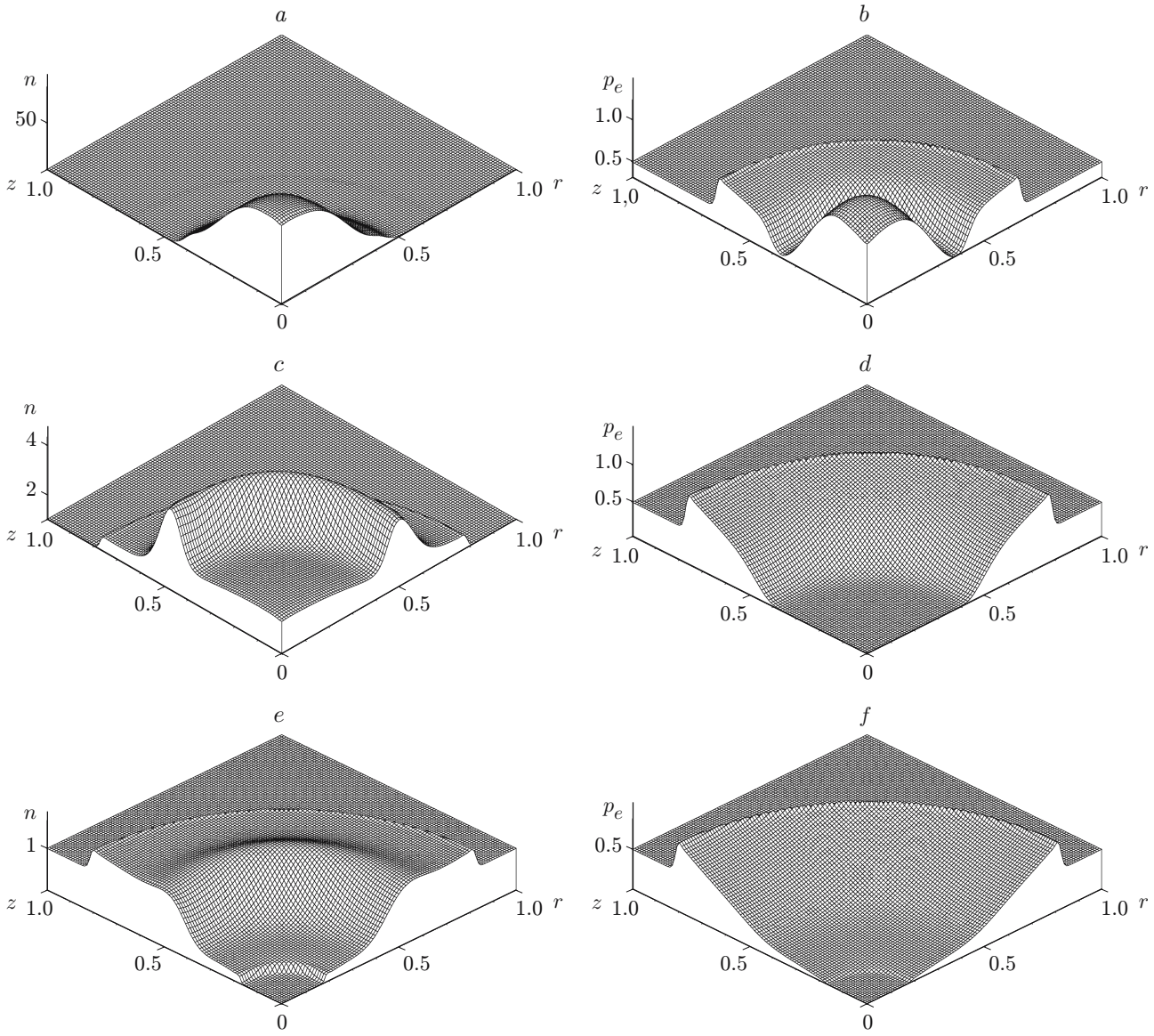

Fig. 1. Distributions of density (a, c, and e) and electron pressure (b, d, and f) for $n_{\rm cl} = 1000$ (a and b), 100 (c and d), and 10 (e and f); $t = 0.3$ and $M_{\rm A} = 0$.

are formed. A region with reduced density (of the order of the background plasma density) and pressure several orders lower than the pressure of the background plasma is formed inside the cloud. The smaller $n_{\rm cl}$, the faster the plasma spread and the lower the plasma density in the center of this region.

Subsequent calculations were performed to study the influence of the magnetic field on propagation of the plasma cloud for different values of $M_{\rm A}$. The magnetic field was directed along the z axis; as a consequence, the magnetic pressure gradient was directed along the radius, which should lead to plasma-cloud compression in the radial direction. Figure 2 shows the plasma spread at the time $t = 0.2$ for $n_{\rm cl} = 1000$ and different values of $M_{\rm A}$. As the magnetic field becomes stronger ($M_{\rm A}$ increases), the plasma spread in the radial direction becomes less intense than that in the longitudinal direction. At $M_{\rm A}^2 = 30$, the plasma spread is almost terminated, and the cloud is divided into two parts moving along the z axis. The amplitudes of density and pressure increase substantially, and the spread velocity in the z direction is independent of the magnetic field. Figure 3 shows the plasma spread at the time $t = 0.15$ for $M_{\rm A}^2 = 5$ and different values of $n_{\rm cl}$. The greater the value of $n_{\rm cl}$, the slower the plasma spread and the lower the plasma density in the center of the region.

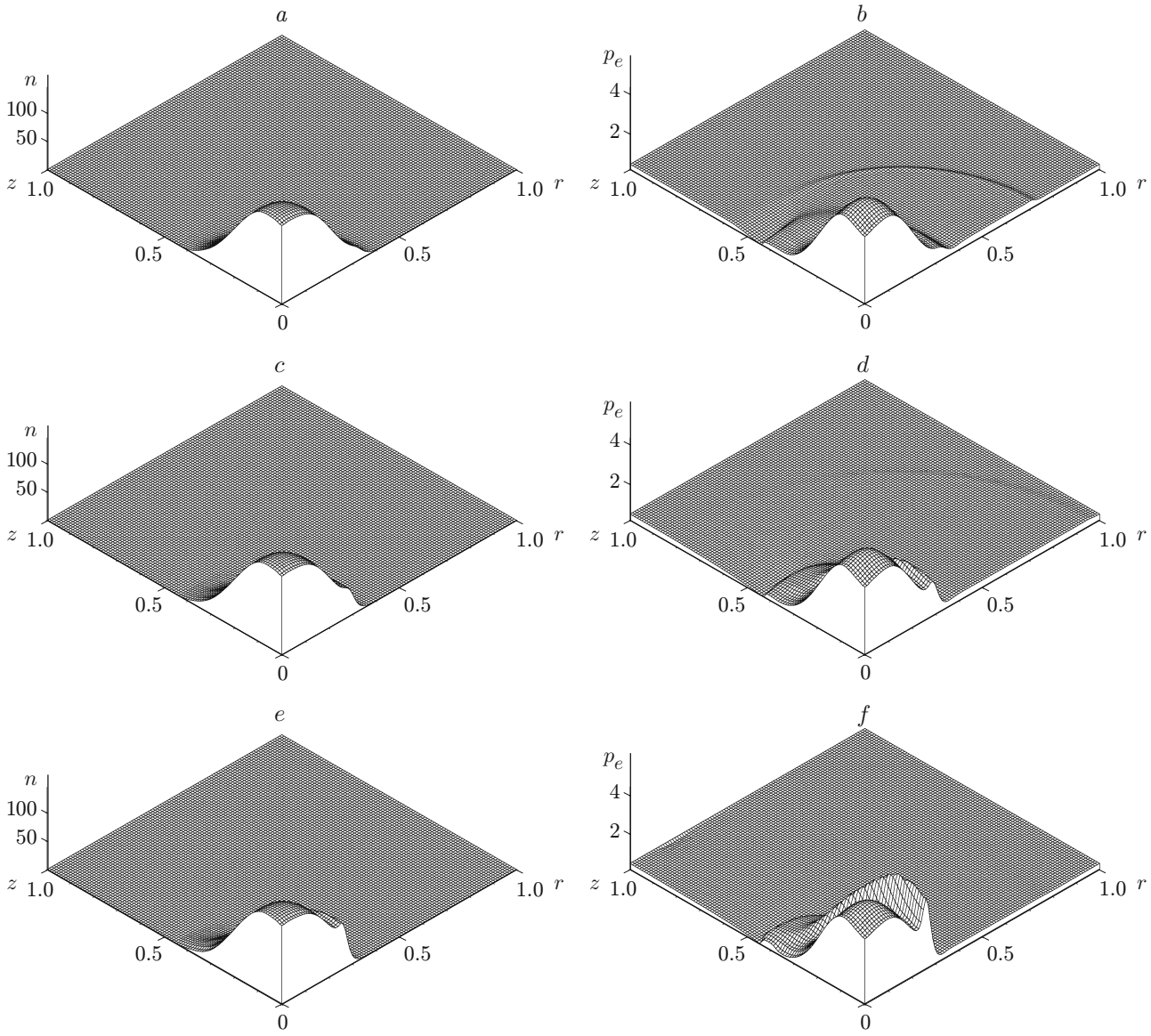

Fig. 2. Distributions of density (a, c, and e) and electron pressure (b, d, and f) for $M_A^2 = 5$ (a and b), 15 (c and d), and 30 (e and f); $t = 0.2$ and $n_{cl} = 1000$.

In the next series of calculations, we studied the influence of nonuniform initial distributions of the electron and ion temperatures on propagation of the plasma cloud into the background plasma. As the equations of motion and magnetic field depend only on the total pressure or the sum of the electron and ion temperatures [see Eq. (2)] rather than on their individual values, the main laws of motion of the plasma cloud also depend only on the summed values of these temperatures. The magnetic field distribution is plotted in Fig. 4.

It follows from Fig. 4 that a magnetic well arises in the center of the cloud. The time of equalization of the ion and electron temperatures in the plasma cloud from their different initial distributions depends substantially on the parameter $k = k_{00}n/\sigma$, i.e., on the "time between collisions" of electrons. For $k_{00} = 8.2$, this time is 0.2, and for $t \geqslant 0.2$ the plasma can be considered as one-fluid and one-temperature. Figure 5 shows the distributions of the electron and ion temperatures on the radial axis ($z = 0$) versus the parameter k_{00}. The greater the value of k_{00}, the faster the electron and ion temperatures become equalized, after which the plasma can be considered as one-fluid and one-temperature.

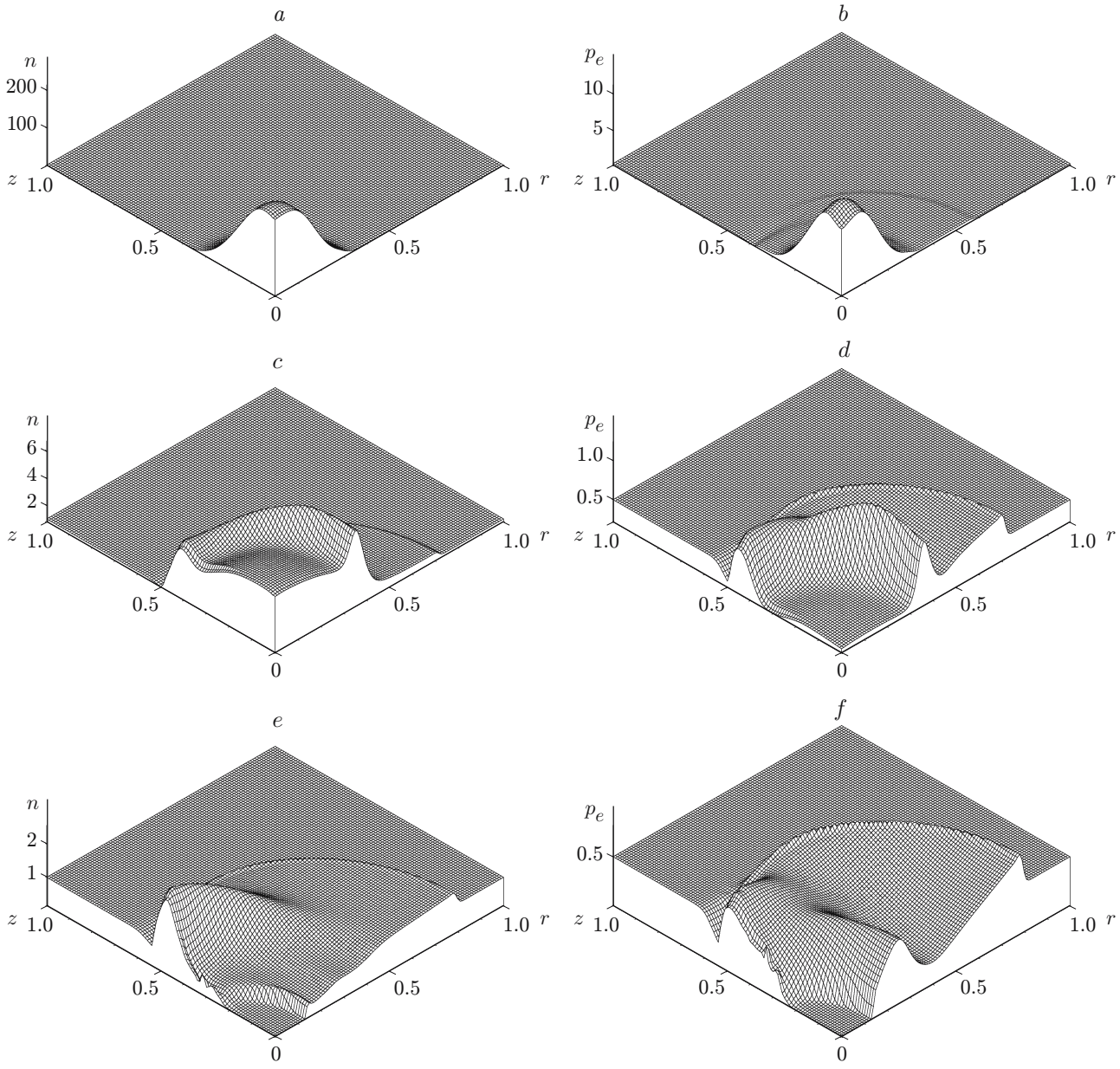

Fig. 3. Distributions of density (a, c, and e) and electron pressure (b, d, and f) for $n_{\rm cl} = 1000$ (a and b), 100 (c and d), and 10 (e and f); $t = 0.15$ and $M_{\rm A}^2 = 5$.

The results of the present calculations offer an adequate description of the physics of the phenomenon under study and are in good qualitative and quantitative agreement with available results of physical and numerical experiments [1–5, 8].

The theoretical analysis and calculations performed confirm the efficiency of the numerical algorithm proposed and the software tools developed on the basis of this algorithm. Hence, it can be used for solving more complicated problems of plasma spreading in a magnetic field with allowance for heat conduction and a finite conductivity of the plasma.

This work was supported by the Russian Foundation for Basic Research (Grant No. 05-01-00146).

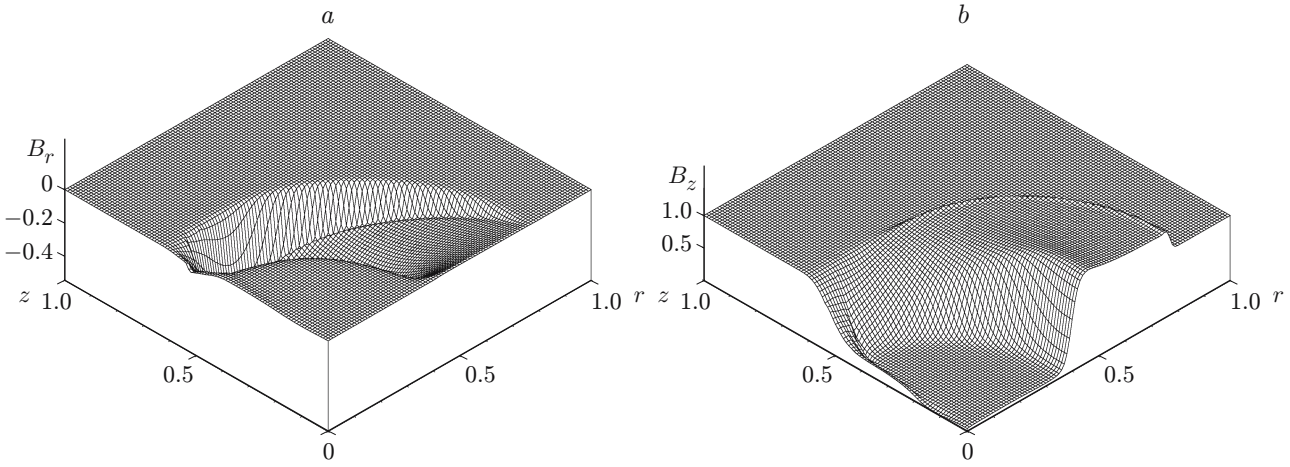

Fig. 4. Distributions of the radial component (a) and z component (b) of the magnetic field for $t = 0.2$, $M_{\rm A}^2 = 5$, $T_{i,\rm cl} + T_{e,\rm cl} = 1$, $p_{i,\rm cl} + p_{e,\rm cl} = 1000$, and $n_{\rm cl} = 1000$.

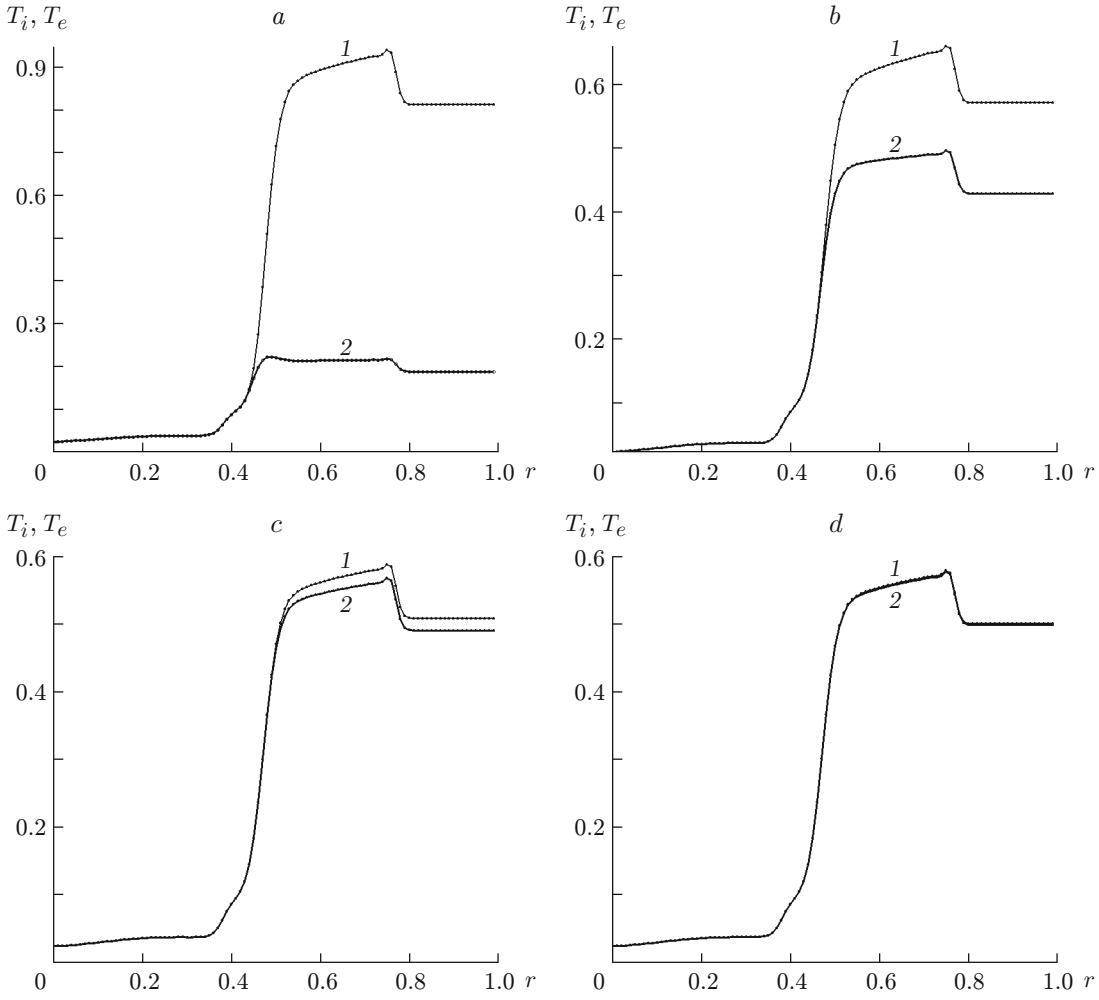

Fig. 5. Distributions of the electron (1) and ion (2) temperatures on the radial axis ($z = 0$) for $k_{00} = 1$ (a), 3 (b), 5 (c), and 7 (d); $t = 0.2$, $p_{i,\rm cl} = 1000$, $p_{e,\rm cl} = 0$, $n_{\rm cl} = 1000$, and $M_{\rm A}^2 = 5$.

REFERENCES

1. A. V. Burdakov, A. V. Arzhannikov, V. T. Astrelin, et al., "Fast heating of ions in GOL-3 multiple mirror trap," in: *Proc. of the 31th Conf. on Controlled Fusion and Plasma Physics* (London, June 28–July 2, 2004) [CD-ROM], Vol. 27A, European Physical Society (2004), p. 4.156.
2. A. V. Arzhannikov, V. T. Astrelin, A. V. Burdakov, et al., "Direct observation of anomalously low longitudinal electron heat conduction during collective relaxation of a high-current relativistic electron beam in the plasma," *Pis'ma Zh. Éksp. Teor. Fiz.*, **77**, No. 7, 426–429 (2003).
3. A. V. Arzhannikov, V. T. Astrelin, A. V. Burdakov, et al. "Dynamics of ions of a beam-heated plasma in a cell of multimirror open trap," *Trans. Fus. Technol.*, **43**, No. 1, 172–176 (2003).
4. V. T. Astrelin, A. V. Burdakov, V. M. Kovenya, and T. V. Kozlinskaya, "Numerical simulation of plasma dynamics in a nonuniform magnetic field," *J. Appl. Mech. Tech. Phys.*, **47**, No. 1, 27–35 (2006).
5. V. M. Kovenya and T. V. Kozlinskaya, "Calculation algorithm for electron-beam-induced plasma heating," *Vychisl. Tekhnol.*, **9**, No. 6, 59–67 (2004).
6. V. M. Kovenya and T. V. Kozlinskaya, "Predictor–corrector method for solving problems of magnetic hydrodynamics," *Vychisl. Tekhnol.*, **11**, No. 6, Special Issue, Part 1, 84–93 (2006).
7. S. I. Braginskii, "Transport phenomena in plasma," in: *Problems in Plasma Theory* [in Russian], Vol. 1, Gosatomizdat, Moscow (1963), pp. 183–212.
8. V. T. Astrelin, A. V. Burdakov, N. A. Guber, and V. M. Kovenya, "Simulation of the motion and heating of an irregular plasma," *J. Appl. Mech. Tech. Phys.*, 42, No. 6, 929–931 (2001).